Lattice excitations in icosahedral Al-Mn-Pd and Al-Re-Pd

Ch. Wälti, E. Felder, M. A. Chernikov, and H. R. Ott
Laboratorium für Festkörperphysik, ETH-Hönggerberg, 8093 Zürich, Switzerland

M. de Boissieu
LTPCM/ENSEEG, Boîte Postale 75, 38402 St. Martin d'Hères Cédex, France

C. Janot
Institute Laue Langevin, Boîte Postale 156, 38042 Grenoble Cédex 9, France
(Received 22 August 1997)

We report results of measurements of the specific heat $C_p(T)$ of a large Czochralski-grown single grain of icosahedral $Al_{68.2}Mn_9Pd_{22.8}$ and of a high-quality single-phase sample of icosahedral $Al_{70}Re_{8.6}Pd_{21.4}$ in the temperature range between 1.6 and 280 K. For icosahedral $Al_{68.2}Mn_9Pd_{22.8}$, the cubic-in-T term to the low-temperature specific heat $C_p(T)$ is distinctly larger than the expected acoustic-phonon contribution calculated from the results of low-temperature measurements of the sound velocities v_l and v_t, thus indicating a large excess specific heat $C_{ex}(T)$. The same conclusion can be reached for $Al_{70}Re_{8.6}Pd_{21.4}$. [S0163-1829(98)02517-X]

I. INTRODUCTION

Since the discovery of highly ordered quasicrystals with face-centered icosahedral symmetry and long-range quasiperiodic order with structural coherence lengths up to 10^4 Å,[1–3] many theoretical and experimental investigations of their dynamical properties have been made. In these materials with long-range orientational order but only quasiperiodic translational order, the common procedures based on periodic boundary conditions for evaluating the lattice and electronic excitation spectra no longer apply. Only in the one-dimensional case, an exact solution of the acoustic eigenmode problem has been found.[4–6] Investigations of the three-dimensional case revealed that eigenstates in quasicrystals are always affected by an intrinsic decay rate and therefore are never strictly localized in k space.[5,7] The intrinsic decay rate varies exponentially with the strength of the quasiperiodic potential and therefore in the long-wavelength limit the intrinsic decay will be overshadowed by other decay mechanisms, such as phonon-phonon scattering due to the anharmonicity of the lattice oscillations. Inelastic neutron-scattering investigations on icosahedral Al-Mn-Pd revealed the existence of well-defined acoustic modes in the vicinity of strong Bragg reflexions. Several other broad dispersionless excitations at various energies up to 23 meV have been observed.[8,9]

The elementary excitations are directly related to the specific heat of a material. Therefore, measurements of the specific heat may serve as a tool for gaining information on the elementary excitation spectrum of a solid. Among thermodynamically stable icosahedral quasicrystals, Al-Mn-Pd is one of the very few systems for which quasicrystals are available as large single grains, and therefore, for Al-Mn-Pd quasicrystals the phonon properties have been investigated in great detail.[8,9] Face-centered icosahedral Al-Re-Pd can be obtained in the form of polygrained specimens which show, depending on the composition, very low electrical conductivities at low temperatures, comparable to those observed in doped semiconductors.[10] Since no magnetic excitations are present at low temperatures, a precise evaluation of the lattice contribution to the total measured specific heat can be achieved. Therefore, Al-Re-Pd may be considered as a model system for the investigation of nontrivial thermodynamic properties of nonperiodically structured materials.

No measurements of the specific heat in a wide temperature range up to room temperature have, to our knowledge, been reported for the face-centered icosahedral quasicrystals of the Al-Mn-Pd and Al-Re-Pd alloy systems. Below we present the results of measurements of the specific heat $C_p(T)$ of a high-quality single grain of an icosahedral $Al_{68.2}Mn_9Pd_{22.8}$ quasicrystal, of a polygrain quasicrystal with the composition $Al_{70}Mn_9Pd_{21}$, and of a large bulk sample of icosahedral $Al_{70}Re_{8.6}Pd_{21.4}$, covering the temperature range between 1.6 and 300 K. Parts of these results, particularly those for $C_p(T)$ below 15 K have been reported in previous publications.[11,12]

II. SAMPLES AND EXPERIMENTS

The single grain of icosahedral $Al_{68.2}Mn_9Pd_{22.8}$ was grown with the Czochralski method from a melt of initial composition 72.1 at.% Al, 20.7 at.% Pd, and 7.2% Mn. The details of the sample preparation are described elsewhere.[13] The specimen has been checked by scanning electron microscopy (SEM) investigations and electron-probe microanalysis and was found to consist of one single phase. X-ray energy-dispersive spectroscopy yielded the final composition 68.2 at.% Al, 22.8 at.% Pd, and 9 at.% Mn. The homogeneity and single quasicrystallinity was checked by x-ray Laue diffraction at different orientations. The full width at half maximum of the sharp Bragg reflexions is limited by the instrumental resolution and corresponds to a correlation length of several tenth of μm. Transmission electron microscopy (TEM) investigations revealed a very high de-

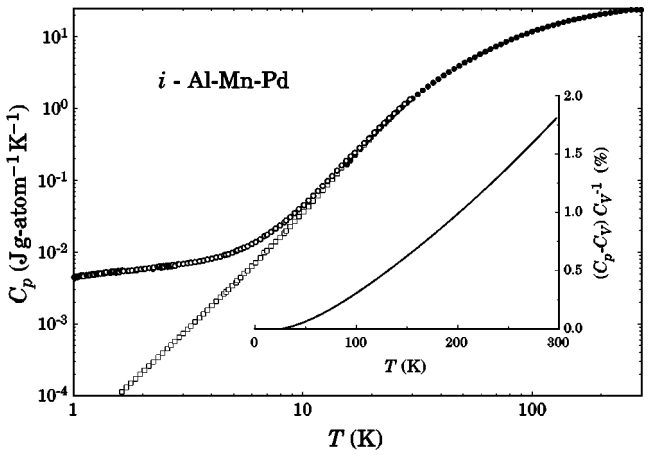

FIG. 1. Specific heat $C_p(T)$ of icosahedral $Al_{68.2}Mn_9Pd_{22.8}$ as a function of temperature between 1.6 and 280 K. The full circles correspond to the specific heat of the single grain of $Al_{68.2}Mn_9Pd_{22.8}$ and the empty circles to the polygrained sample (see text). The empty squares indicate the lattice contribution to the specific heat at low temperatures (see text). The inset shows the calculated difference between $C_p(T)$ and $C_V(T)$, due to thermal-expansion effects, as a function of temperature (see text).

gree of structural perfection of the quasicrystal with negligible phason strains and confirmed the absence of precipitates of other phases.[13]

The polygrain specimen of icosahedral $Al_{70}Mn_9Pd_{21}$ was synthesized from 99.997% pure aluminum, 99.9+% pure palladium, and 99.94% pure manganese. To provide homogeneity, the sample was arc melted several times and subsequently quenched into water directly from 800 °C. The details of the sample preparation and the $C_p(T)$ measurements have been reported elsewhere.[11]

The sample of icosahedral $Al_{70}\,Re_{8.6}\,Pd_{21.4}$, synthesized from 99.999% pure aluminum, 99.9975% pure palladium, and 99.94% pure rhenium, was arc-melted several times, annealed and subsequently rapidly cooled to room temperature. The details of the sample preparation were presented in Ref. 12. The x-ray powder patterns contained no traces of other phases and the SEM investigation using backscattered images did not reveal any mass contrast, thus confirming the homogeneity of our sample. The selected-area electron-diffraction patterns confirmed a high degree of quasiperiodic order and a very low density of phason defects.

The specific heats $C_p(T)$ of these samples were measured using two different experimental techniques in overlapping temperature ranges. A standard relaxation technique was employed in the temperature range between 1.6 and 30 K. For temperatures between 15 and 300 K an adiabatic continuous-heating calorimeter was used. Special care was taken to minimize the radiation losses at elevated temperatures.[14] The temperatures in the range between 1.6 and 30 K were reached using a pumped ^{4}He cryostat, and for those between 15 and 300 K, a conventional gas-flow ^{4}He cryostat was used.

III. RESULTS AND DISCUSSION

A. Icosahedral Al-Mn-Pd

In Fig. 1 the measured total specific heat $C_p^{sg}(T)$ of a single grain of icosahedral $Al_{68.2}Mn_9Pd_{22.8}$ is shown as a function of temperature on logarithmic scales for the temperature range between 12 and 300 K. In the same figure, we show the measured total specific heat $C_p^{pg}(T)$ of the high-quality polygrained sample of icosahedral $Al_{70}Mn_9Pd_{21}$ in the temperature range between 1.6 and 18 K. We note that the $C_p^{sg}(T)$ and $C_p^{pg}(T)$ data coincide in the overlap temperature range. Therefore we assume with some confidence that the low-temperature data of the polygrained sample also represents the specific heat of the single grain material. The open squares in Fig. 1 represent the remaining specific heat $C_p'(T)$ obtained by subtracting off estimates of the magnetic contribution $C_m(T)$, and the electronic and tunneling states contribution $(\gamma_{el}+\gamma_{TS})\,T$ from the total measured specific heat. The evaluation of these terms is explained in detail in previous work.[11] At temperatures near 300 K, the measured specific heat C_p is close to the Dulong-Petit expectation for C_{ph}^V, the specific heat due to lattice excitations at constant volume. At high temperatures, dilatation effects cannot be neglected, and therefore C_{ph}^V may differ substantially from C_{ph}^p, the lattice specific heat at constant pressure.

In order to evaluate the difference between $C_{ph}^p(T)$ and $C_{ph}^V(T)$ for icosahedral $Al_{68.2}Mn_9Pd_{22.8}$, we recall that $C_{ph}^p(T)$ is related to $C_{ph}^V(T)$ as

$$\frac{C_{ph}^p}{C_{ph}^V}-1=3\alpha G T, \tag{1}$$

where α is the linear thermal-expansion coefficient and G is the Grüneisen constant related to the bulk modulus K as

$$G=\frac{1}{2}\left[\left(\frac{\partial K}{\partial p}\right)_T-1\right]. \tag{2}$$

We have calculated the ratio $C_{ph}^p(T)/C_{ph}^V(T)$ for icosahedral $Al_{68.2}\,Mn_9\,Pd_{22.8}$ using $(\partial K/\partial p)_T$ as deduced from the results of measurements of the elastic properties of a single grain of icosahedral Al-Mn-Pd reported in Ref. 15, and the linear thermal-expansion coefficient α reported in Ref. 16, including additional unpublished data.[17] The result of this calculation is displayed in the inset of Fig. 1 as the plot of $(C_{ph}^p/C_{ph}^V)-1$. We note that the relative difference between the measured specific heat C_{ph}^p and the calculated values of C_{ph}^V does not exceed 2% over the whole temperature range covered in this experiment.

1. Specific heat and vibrational excitations at low temperatures ($T<15$ K)

We first focus on the low-temperature variation of $C_{ph}^p(T)$ where any difference to C_{ph}^V may safely be neglected. Below, we use C_{ph} for C_{ph}^p, the lattice specific heat at constant pressure p. The behavior of the specific heat C_{ph} of periodic crystals for temperatures $T<0.02\theta_D$, where θ_D is the Debye temperature at very low temperatures, is well described by the Debye model, i.e., assuming no dispersion in the vibrational excitation spectrum. For periodic crystals this assumption is well justified in the long-wavelength limit, i.e., when $\lambda_{ph}\gg a$, where a is the lattice parameter. Although for quasicrystals no strict definition of a three-dimensional lattice

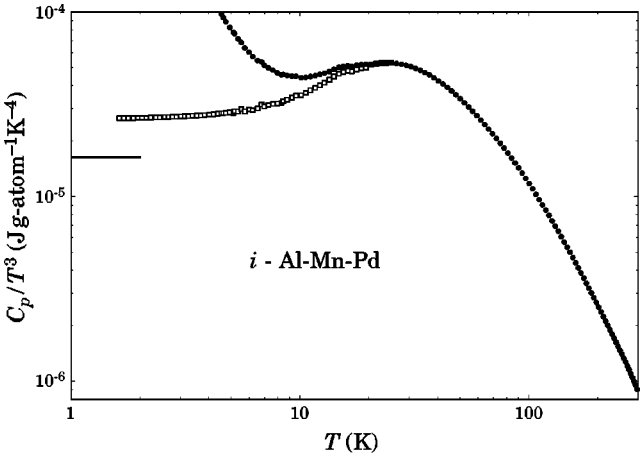

FIG. 2. Specific heat of icosahedral $Al_{68.2}Mn_9Pd_{22.8}$ plotted as $C_p(T)/T^3$ versus T (full circles). The empty squares represent the lattice contribution at low temperatures (see text). The horizontal solid line indicates the Debye specific heat C_D/T^3, calculated from measured sound velocities using Eq. (3).

parameter is possible, we expect, that also for them the Debye-type approximation holds when $\lambda_{ph} \gg b$, where b is the characteristic size of the structural motif. A natural choice for b in icosahedral quasicrystals is the diameter of an icosahedral cluster which is of the order of 20 Å.[18]

In Fig. 2 we show the measured specific heat of $Al_{68.2}Mn_9Pd_{22.8}$ plotted as C_p/T^3 vs T as full circles. The open squares represent C_p'/T^3. From the plot of the ratio C_p'/T^3 versus temperature it is possible to identify the deviations from the low-temperature Debye-type behavior

$$C_D(T) = \frac{2\pi^2 k_B^4}{5\hbar^3 v_s^3}\ T^3. \tag{3}$$

Here v_s is the weighted average

$$\frac{3}{v_s^3} = \frac{1}{v_l^3} + \frac{2}{v_t^3} \tag{4}$$

of the sound velocities v_l and v_t for the longitudinal and shear waves, respectively. Using the low-temperature values of v_l and v_t reported in Ref. 15 we obtain $v_s = 4.09 \times 10^5$ cm s^{-1} for the average sound velocity of icosahedral $Al_{68.2}Mn_9Pd_{22.8}$. This value v_s is compatible with $C_D/T^3 = 1.63 \times 10^{-5}$ J g-atom^{-1} K^{-4}, which is indicated as a short horizontal solid line at the left margin of Fig. 2. We conclude that for icosahedral Al-Mn-Pd, the cubic-in-T term to the specific heat, represented by the empty squares in Fig. 2, is, in the limit of low temperatures, distinctly larger than the Debye value C_D/T^3 calculated from results of acoustic measurements, suggesting a large excess T^3 term to the specific heat.

Large excess specific heats C_{ex} of the lattice are very common in amorphous solids. It has been suggested that for these materials stationary anharmonic resonant modes may contribute a distinct excess cubic-in-T term to the specific heat.[19] The eigenvalue equation for the anharmonic resonant mode is similar to that obtained for a harmonic resonant mode produced by a force-constant defect,[20] and therefore the low-frequency density of states (DOS) is proportional to ω^2. For icosahedral quasicrystals with face-centered icosahedral structures, such as Al-Mn-Pd or Al-Re-Pd, it was argued[21] that the phonon-phason coupling may lead, in the presence of large phason strain, to a softening of shear acoustic waves and consequently to an increase of the cubic-in-T term to $C_p(T)$. TEM investigations of our $Al_{68.2}Mn_9Pd_{22.8}$ quasicrystal, however, revealed negligible phason strain, and therefore the phason-phonon hypothesis is not an obvious choice for explaining our observation.

As an alternative explanation we consider that the excess cubic-in-T term to $C_p(T)$ of icosahedral quasicrystals might be of electronic origin. Icosahedral quasicrystalline phases are thought to be stabilized through a Hume-Rothery-type mechanism, related with a pseudogap in the electronic DOS at the Fermi energy E_F.[22] Electronic structure calculations for rational approximants of various icosahedral quasicrystals and various types of experiments reveal a depression of the electronic DOS at E_F.[23–26] The calculations predict that the structure of the electronic DOS, even inside the pseudogap, is modulated by a set of narrow spiky peaks with a width of less than 10 meV.[27]

The contribution of electronic excitations to the specific heat is given by

$$C_{el} = \frac{\partial}{\partial T}\int_0^\infty dE f(E,T) D(E) E, \tag{5}$$

where $f(E,T)$ is the Fermi-Dirac function and $D(E)$ is the electronic DOS. Using the Sommerfeld expansion, Eq. (5) reduces to

$$C_{el} = \gamma T + \beta_{el} T^3 + O(T^5), \tag{6}$$

where the Sommerfeld constant γ and β_{el} are given by

$$\gamma = \frac{\pi^2}{3} k_B^2 D(E_F) \tag{7a}$$

and

$$\beta_{el} = -\frac{\pi^4}{90} k_B^4 D(E_F)\left[15\left(\frac{D'(E_F)}{D(E_F)}\right)^2 - 21\frac{D''(E_F)}{D(E_F)}\right]. \tag{7b}$$

Here, D' and D'' are the first and the second derivatives of the electronic DOS with respect to the energy, respectively. This approximation holds as long as $k_B T \ll E_0$, where E_0 describes the characteristic energy scale over which $D(E)$ changes significantly.

In conventional metals, $D(E)$ is a slowly varying function of E near E_F, therefore both D' and D'' are small and the T^3 correction to the usual electronic specific heat γT can be neglected. For icosahedral quasicrystals, however, a strong variation of the electronic DOS close to the Fermi energy[23–27] may lead to large values of $D'(E_F)$ and $D''(E_F)$, and consequently to large values of β_{el}. Although no experiment has, so far, given a clear indication of the spiky features in the electronic DOS, we present below a crude estimate of the possible influence of narrow structures in the electronic DOS on $C_p(T)$.

Consider a parabolicly shaped minimum in the electronic DOS at the Fermi energy of the form

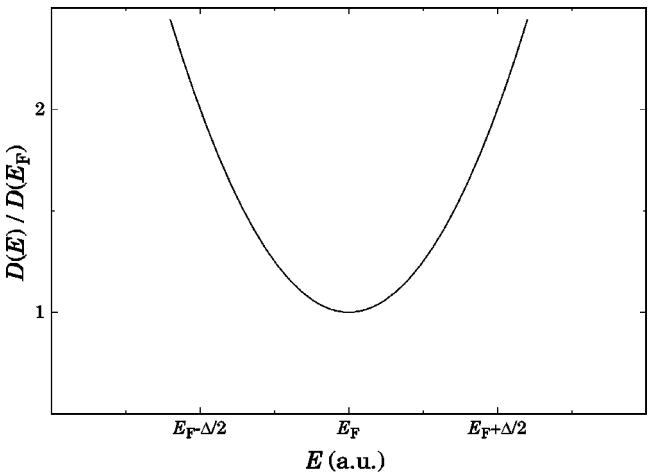

FIG. 3. Electronic model DOS $D(E)$ near E_F.

$$D(E)=D(E_F)\left[1+\left(\frac{E-E_F}{\Delta}\right)^2\right] \tag{8}$$

with a width Δ of 5 meV (see Fig. 3). The second derivative of the electronic DOS given by Eq. (8) leads, using Eq. (7b), to a T^3 term to the electronic specific heat $C_{\rm el}$, that is of the same order of magnitude as the cubic-in-T excess specific heat $C_{\rm ex}$ of icosahedral $Al_{68.2}Mn_9Pd_{22.8}$.

Various experiments probing $D''(E_F)$ (Refs. 28–31) have indicated, however, that the $D''(E_F)/D(E_F)$ ratios are substantially smaller than those which are compatible with the assumption that the observed excess specific heat is of electronic origin. Among those are ^{27}Al NMR experiments,[28–30] probing the temperature dependence of the spin-lattice relaxation-rate in various icosahedral quasicrystals, which have indicated strong deviations from the usual Korringa-type relaxation behavior $(T_1T)^{-1}=$const. observed in metals. The temperature dependence of the spin-lattice relaxation rate T_1, including terms to order T^3, is of the form[32]

$$\frac{1}{T_1T}\propto(1+\epsilon T^2), \tag{9}$$

where ϵ is given by

$$\epsilon=\frac{\pi^2k_B^2}{3}\frac{D''(E_F)}{D(E_F)}. \tag{10}$$

The $D''(E_F)/D(E_F)$ ratios that are compatible with the results of the mentioned experiments[28–30] account for only a few percent of the observed cubic-in-T excess specific heat, indicating that most likely $C_{\rm ex}$ for the most part is of nonelectronic origin.

In what follows we therefore consider that $C_{\rm ex}$, the difference between $C_p'(T)$ and C_D is caused by an enhanced lattice contribution, exceeding the expected acoustic specific heat. In Fig. 4 we show $C_p'/T^3=C_{\rm ph}/T^3$ vs T^2 in the temperature range between 1.6 and 14 K. The data are very well represented by an expression of the form

$$C_{\rm ph}=\beta T^3+\delta T^5, \tag{11}$$

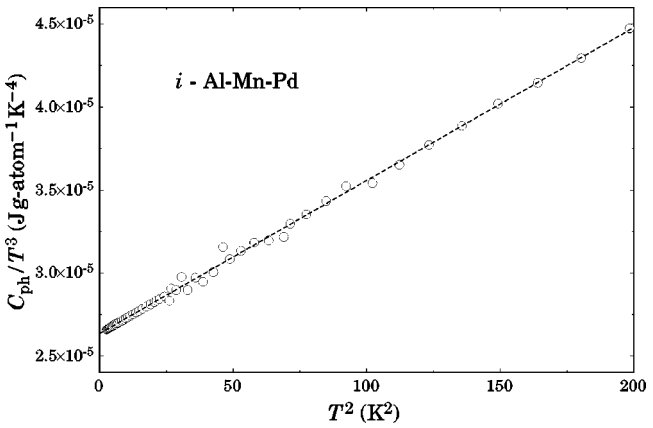

FIG. 4. Lattice contribution to the specific heat of icosahedral $Al_{68.2}Mn_9Pd_{22.8}$ plotted as $C_{\rm ph}(T)/T^3$ versus T^2 at low temperatures. The broken line is a fit of Eq. (11), as explained in text.

with the parameters $\beta=2.63\times10^{-5}$ J g-atom^{-1} K^{-4} and $\delta=9.21\times10^{-8}$ J g-atom^{-1} K^{-6} as may be seen by the broken line in Fig. 4.

The contribution of lattice vibrational excitations to the specific heat is given by

$$C_{\rm ph}(T)=\int d\omega\; g(\omega)\frac{\partial}{\partial T}\left(\frac{\hbar\omega}{\exp(\hbar\omega/k_BT)-1}\right), \tag{12}$$

where $g(\omega)$ is the density of vibrational states (DOVS). The temperature dependence of the low-temperature lattice specific heat $C_{\rm ph}(T)$ given by Eq. (11) is compatible with the low-frequency part of a DOVS of the form

$$g(\omega)=\begin{cases}a\omega^2+b\omega^4 & \text{for } \omega\leqslant\omega_0\\ 0 & \text{for } \omega>\omega_0.\end{cases} \tag{13}$$

The substitution of Eq. (13) into Eq. (12) leads to a specific heat $C_{\rm ph}(T)$ of the same form as given in Eq. (11) with

$$\beta=\left[9N_A\left(\frac{k_B}{\hbar\omega_0}\right)^3-\frac{3b}{5}\omega_0^2\left(\frac{k_B}{\hbar}\right)^3\right]\frac{4k_B\pi^4}{15} \tag{14a}$$

and

$$\delta=6\hbar b\left(\frac{k_B}{\hbar}\right)^6\frac{8\pi^6}{63}, \tag{14b}$$

where ω_0 is given by

$$3N_A=\frac{a}{3}\omega_0^3+\frac{b}{5}\omega_0^5. \tag{14c}$$

Thus, the lattice specific heat as given by Eqs. (11) and (14a)–(14c) assuming a DOVS as given in Eq. (13) describes the measured $C_{\rm ph}/T^3$ vs T curve at low temperatures very well (see Fig. 4). Both the upturn of the ratio $C_{\rm ph}/T^3$ and the subsequent maximum in $C_{\rm ph}/T^3$ are common for amorphous solids,[33] but have also been observed in highly ordered crystals with low-lying optical phonons.[34,35] This deviation of the specific heat ratio $C_{\rm ph}/T^3$ at low temperatures from a constant value that is expected in the Debye-type approximation, is most likely caused by a deviation of the dispersion relation $\omega(k)$ of the lowest transverse-acoustical branches from the linear variation $\omega\propto k$. In a first approxi-

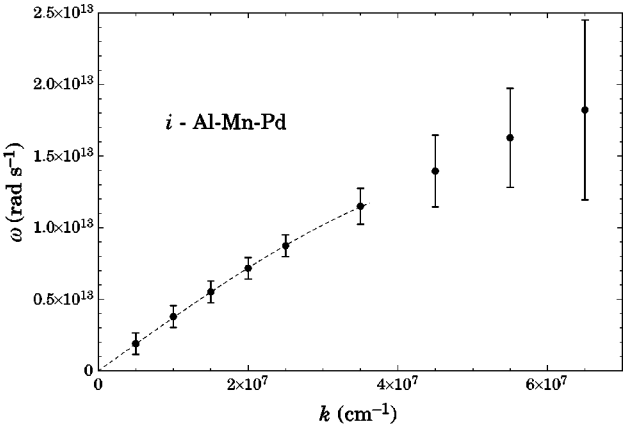

FIG. 5. Dispersion relation of the transverse acoustic excitations of icosahedral Al-Mn-Pd measured at 300 K (Ref. 41). The broken line is a fit of Eq. (15) to the data.

mation the dispersion relation $\omega(k)$ of the transverse acoustical excitations can be expanded in a power series of the form

$$\omega(k)=v_t k+\alpha k^3. \tag{15}$$

For most solids the coefficient α is negative.[36] This simply reflects the fact that the group velocity of the lattice excitations decreases with increasing k. For some periodic crystals, however, the coefficient α is positive. Examples are the A15 compound Nb_3Sn (Ref. 37) and Nb metal.[38] For these materials with strong electron-phonon interaction, the unusual $\omega(k)$ variation is thought to arise from the complex interplay of interatomic elastic forces.[39]

The increase of the C_{ph}/T^3 vs T curve could also be caused by contributions from low-energy optical phonons. For example, numerical calculations by de Wette and Kulkarni[40] revealed a contribution to the specific heat of $YBa_2Cu_3O_7$ from dispersionless excitations with energies $\nu=2\times10^{12}$ Hz already at 6 K, where C_{ph}/T^3 starts to increase considerably with increasing temperature.

In Fig. 5, we show the dispersion relation of the lowest phonon branch of $Al_{68.2}Mn_9Pd_{22.8}$ measured at $T=300$ K by de Boissieu[41] using inelastic neutron scattering. Measurements of the sound velocities at temperatures between 300 and 4 K by Amazit *et al.*[15] revealed only small variations of v_t and v_l upon cooling, of the order of a few percent. Therefore, we assume that in the temperature range between 1 and 300 K the coefficients of the dispersion relation do not change significantly. In icosahedral quasicrystals, the lowest phonon branch is transversal and doubly degenerate for any direction of the wave vector **k**. According to the previously established ratio $v_l/v_t=1.8$,[15] the transverse modes of acoustical excitations contribute more than 90% to the cubic-in-T term of the specific heat due to acoustic degrees of freedom. Therefore, we can estimate the specific heat due to acoustic excitations below 5 K using the dispersion relation shown in Fig. 5 within a few percent.

A fit of Eq. (15) to the $\omega(k)$ data, indicated as a broken line in Fig. 5, yields the coefficient $\alpha=(-3.9\pm0.1)\times10^{-11}$ cm^3 s^{-1} for the cubic-in-k term and $v_t=(3.75\pm0.1)\times10^5$ cm s^{-1}. In the acoustical limit, the dispersion relation $\omega(k)$ for quasicrystals with an icosahedral point-group symmetry depends only on the absolute value of **k**, leading to a DOVS of the acoustic modes of the form described by Eq. (13), where the ω^4 term is given by

$$g_4(\omega)=g_{4t}(\omega)+g_{4l}(\omega)=-\left(\frac{5\alpha_t}{\pi^2 v_t^6}+\frac{5\alpha_l}{2\pi^2 v_l^6}\right)\omega^4. \tag{16}$$

According to neutron-scattering experiments on other quasicrystals, the parameters α_t and α_l are of comparable magnitude.[42] Therefore, the longitudinal term in Eq. (16) does not exceed a few percent of the transversal contribution. Inserting the parameters α_t and v_t, obtained as described above, yields the parameters $a=1.8\times10^{-17}$ s^3 g-atom^{-1} and $b=6.5\times10^{-44}$ s^5 g-atom^{-1} of Eq. (13). Inserting a and b into Eqs. (14a)–(14c) leads to $\delta=2.5\times10^{-8}$ J g-atom^{-1} K^{-6} that is distinctly smaller than the corresponding value $\delta=9.2\times10^{-8}$ J g-atom^{-1} K^{-6} obtained from the fit of Eq. (11) to the low-temperature specific heat, suggesting the presence of a large T^5 excess specific heat that is of nonacoustic origin.

2. Density of vibrational states

In principle, the DOVS can directly be evaluated from results of inelastic neutron-scattering experiments. For nonmonoatomic materials, however, these measurements provide a generalized density of vibrational states (GDOVS), which is a normalized sum of the partial DOVS, weighted with the Debye-Waller factor, the concentration, the scattering cross section, and the atomic mass of each element in the sample. For Al-Mn-Pd materials, the corresponding weights are fairly close to each other[43] and in this particular case in the limit of low frequencies, the GDOVS is expected to be close to the DOVS. The resolution of these experiments depends on the energy and it decreases substantially for vibrational excitation energies below ≈20 meV. In the low-energy range, which cannot be accessed by neutron-scattering experiments, the DOVS can, however, be calculated from the low-temperature specific-heat data. In Fig. 6 we show the GDOVS as a function of energy as derived from inelastic neutron-scattering data.[44] This GDOVS was extrapolated to the energy range between 0 and 8 meV, i.e., $0<\omega<1.215\times10^{13}$ s^{-1}, by using the proportionality $g(\omega)\sim\omega^2$. Using Eq. (12), we have calculated the specific heat $C_{ph}(T)$ inserting for $g(\omega)$ the GDOVS as it follows from Ref. 44. The result of this calculation is represented by the solid line in the inset of Fig. 6. Below 20 K, the lattice specific heat $C_{ph}(T)$ obtained from the *measured* $C_p(T)$ data in the way described above, is distinctly smaller than the result of this calculation. This implies that the low-frequency part of the GDOVS of Ref. 44 is not compatible with the measured $C_{ph}(T)$ at low temperatures and we briefly discuss this discrepancy below. Similarly, the average sound-velocity deduced from the measured GDOVS, using the Debye-type low-frequency proportionality $g(\omega)\sim v_s^{-3}\omega^2$ differs substantially from the average sound-velocity measured at low temperatures.[15]

Although Eq. (12) relates C_{ph} with $g(\omega)$, the DOVS cannot be evaluated from the measured specific heat in an unambiguous way. Nevertheless, because at low temperatures

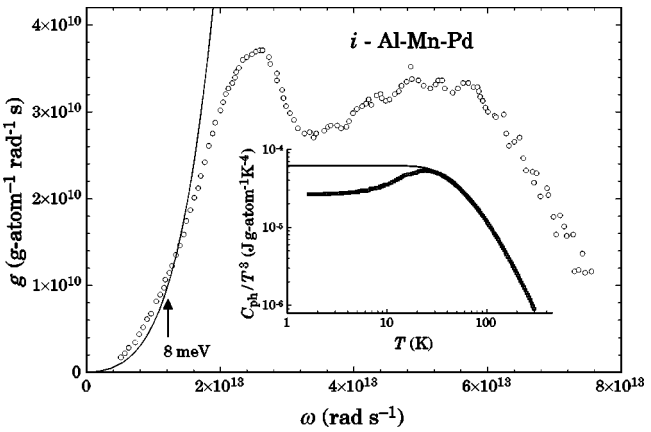

FIG. 6. Generalized density of vibrational states (GDOVS) of icosahedral $Al_{71}Mn_{10}Pd_{19}$ per unit of frequency and per g-atom (from Ref. 44). The solid line indicates the low-frequency DOVS, as calculated from the low-temperature lattice specific heat (see text). The inset shows the lattice specific heat of icosahedral $Al_{68.2}Mn_9Pd_{22.8}$ plotted as $C_{ph}(T)/T^3$ versus T (empty squares). The solid line indicates the specific heat calculated from the GDOVS derived from neutron scattering experiments (Ref. 44) using Eq. (12).

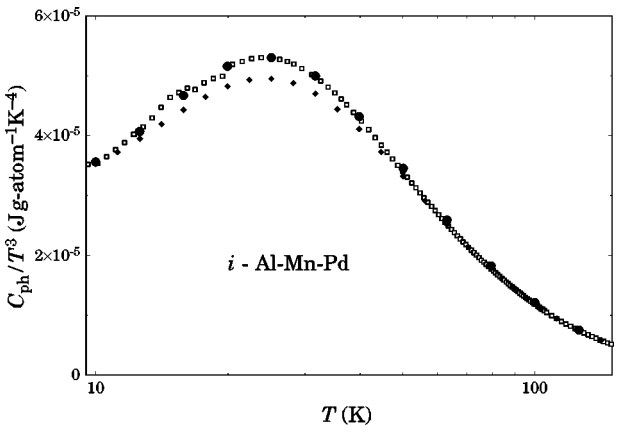

FIG. 7. Lattice contribution to the specific heat of icosahedral $Al_{68.2}Mn_9Pd_{22.8}$ divided by T^3 versus T (empty squares). The ratio $C_{ph}(T)/T^3$, calculated using the GDOVS from Ref. 44, modified at low temperatures (see text and Fig. 6), is shown by full diamonds. The full circles indicate the calculated $C_{ph}(T)/T^3$ ratio using the modified GDOVS and taking into account an additional, dispersionless optical mode (see text).

only the low-frequency part of the DOVS contributes significantly to the specific heat $C_{ph}(T)$, the deviation of the specific heat C_{ph} from the simple T^3 dependence of Eq. (3) can be used to evaluate the deviation of the frequency dependence of the DOVS from the ω^2 Debye-type spectrum at low frequencies.

Fitting the measured specific heat $C_{ph}(T)$ with Eq. (11) provides the two parameters β and δ. Inserting these parameters into Eqs. (14a)–(14c) yields $a=3.27\times10^{-17}$ s^3 g-atom^{-1} and $b=2.37\times10^{-43}$ s^5 g-atom^{-1}. With these parameters, Eq. (13) leads to the low-frequency DOVS that is drawn as a solid line in Fig. 6. The result of this calculation is substantially different from the GDOVS derived from inelastic neutron-scattering data,[44] which is most likely caused by the limited accuracy of the neutron time-of-flight technique at low frequencies.

3. Intermediate temperatures (15 K<T<50 K)

We now turn to the behavior of $C_{ph}(T)$ at intermediate temperatures, where C_{ph}/T^3 increases slowly with increasing temperature and passes over a broad maximum centered at approximately 25 K. In Fig. 7 we show the specific-heat ratio $C_{ph}(T)/T^3$ vs temperature between 10 and 200 K as obtained from experiment (empty squares). The full diamonds display the same ratio that results from calculating the lattice specific heat using Eq. (12) by inserting the low-frequency DOVS as obtained from the low-temperature part of $C_{ph}(T)$ complemented by the GDOVS of Ref. 44 for frequencies exceeding 1.21×10^{13} s^{-1}. The agreement at high temperatures ($T>50$ K) is quite good. It may be seen, however, that the augmented DOVS still cannot explain the height of the broad maximum of C_{ph}/T^3.

Theoretical investigations of the lattice dynamics of rational approximants to icosahedral quasicrystals predict the existence of a hierarchy of nondispersive stationary modes around high-symmetry points corresponding to quasi-Brillouin-zone boundaries.[45] Inelastic neutron-scattering measurements on a single grain of icosahedral $Al_{68.2}Mn_9Pd_{22.8}$ revealed, besides acoustic modes, the existence of a series of broad, 4 meV wide, dispersionless modes at various energies up to 23 meV.[8,9] Dispersionless phonon modes in icosahedral $Al_{68.2}Mn_9Pd_{22.8}$ have also been indicated by optical experiments.[46]

The specific-heat ratio C_{stat}/T^3 of a nondispersive stationary mode with frequency ω shows, as a function of T, a maximum at $T_{max}\approx0.2\hbar\omega/k_B$. With this in mind we have calculated the specific heat $C_{ph}(T)$ using the same procedure as described above, but by taking into account an additional low-energy optical mode in the DOVS. The result is shown as full circles in Fig. 7. It may be seen that at intermediate temperatures ($T\approx25$ K) the agreement between calculation and experiment may substantially be improved. This, in turn, suggests the presence of optical modes at low energies. The present calculation of $C_{ph}(T)$ is based on assuming an additional broad optical mode at an energy of 10 meV with a width of 1 meV.

B. Icosahedral Al-Re-Pd

The complete set of our specific-heat data $C_p(T)$ of icosahedral $Al_{70}Re_{8.6}Pd_{21.4}$ as a function of temperature is shown in Fig. 8 on double logarithmic scales for the whole temperature range covered in this work. The low-temperature part of these data in the range between 0.065 and 18 K has previously been reported in Ref. 12. At the lowest temperatures, the specific heat $C_p(T)$ is dominated by a nuclear hyperfine contribution $C_N=AT^{-2}$. The lattice contribution C_{ph} to the specific heat C_p below 5 K has been evaluated in Ref. 12 by assuming that the main contributions to the specific heat C_p are from nuclear, electronic, tunneling states and lattice excitations

$$C_p(T)=(\gamma_{TS}+\gamma_{el})T+\beta T^3+\delta T^5+AT^{-2}. \qquad (17)$$

The solid line in Fig. 8 indicates a fit of Eq. (17) to the data in the temperature range between 0.065 and 8 K, yielding the

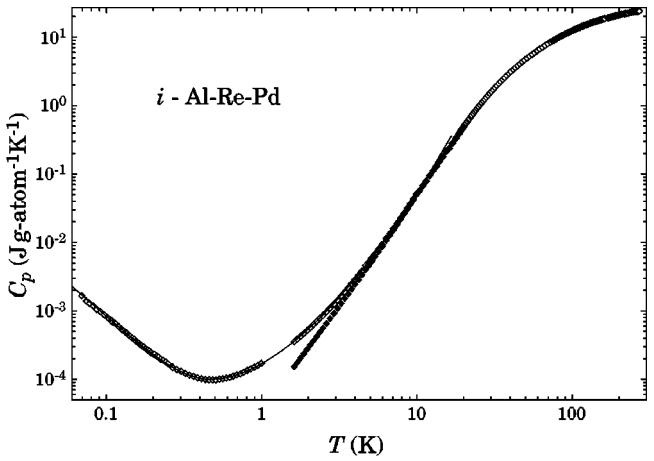

FIG. 8. Specific heat $C_p(T)$ of icosahedral $Al_{70}Re_{8.6}Pd_{21.4}$ as a function of temperature between 0.07 and 280 K (empty diamonds). The full diamonds indicate the lattice contribution to the specific heat at low temperatures. For temperatures above 5 K the linear contribution to the specific heat resulting from the tunneling states and electronic excitations ($\gamma_{el}+\gamma_{TS}$) T is negligible in comparison to the quasilattice contribution (Ref. 12).

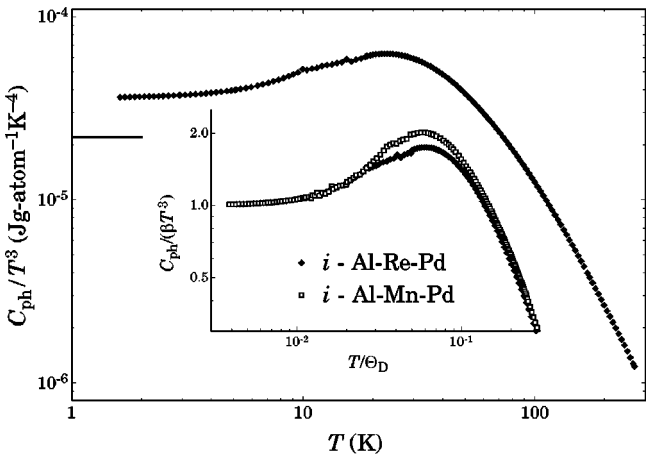

FIG. 9. Lattice contribution to the specific heat $C_{ph}(T)$ of icosahedral $Al_{70}Re_{8.6}Pd_{21.4}$ plotted as C_{ph}/T^3 versus temperature. The horizontal solid line indicates the Debye specific heat C_D/T^3, calculated from estimates of the sound velocities using Eq. (3) (see text). The inset shows the normalized specific-heat ratio $C_{ph}(T)/(\beta T^3)$ versus the normalized temperature (see text) of icosahedral $Al_{70}Re_{8.6}Pd_{21.4}$ (full diamonds) and icosahedral $Al_{68.2}Mn_9Pd_{22.8}$ (empty squares).

parameters $\gamma_{TS}+\gamma_{el}=1.25\times10^{-4}$ J g-atom^{-1} K^{-2}, $A=8.23\times10^{-6}$ J g-atom^{-1} K, $\beta=3.6\times10^{-5}$ J g-atom^{-1} K^{-4}, and $\delta=1.52\times10^{-7}$ J g-atom^{-1} K^{-6}.

The C_N contribution vanishes with increasing temperature as T^{-2} and contributes less than 1% to the total specific heat C_p at temperatures above 1 K. The contributions to the specific heat C_p from the electronic and tunneling states excitations cannot be determined separately. Both terms contribute a linear-in-T term to the specific heat and therefore, the lattice contribution to the specific heat C_p above 1 K can be obtained by subtracting off a linear term. The result of this evaluation of the quasilattice contribution to the specific heat C_{ph} is indicated by full diamonds in Fig. 8. We note that for temperatures between 5 and 300 K, the contribution to the specific heat varying linearly with T does not exceed 1% of the total specific heat.

For icosahedral $Al_{70}Re_{8.6}Pd_{21.4}$, the measured specific heat $C_p(T)$ at the highest temperatures reached in our experiment, is again close to the Dulong-Petit expectation. For this quasicrystalline material the difference between C_{ph}^V and C_{ph}^p cannot be evaluated in simple ways, because neither thermal expansion nor compressibility data are available at present. Since the structure of icosahedral $Al_{70}Re_{8.6}Pd_{21.4}$ is similar to that of icosahedral $Al_{68.2}Mn_9Pd_{22.8}$, there are no reasons to expect the dilatation and compressibility effects of icosahedral $Al_{70}Re_{8.6}Pd_{21.4}$ to be substantially different from those of icosahedral $Al_{68.2}Mn_9Pd_{22.8}$. Thus, we assume the difference between C_{ph}^V and C_{ph}^p to be of the same order of magnitude as in icosahedral $Al_{68.2}Mn_9Pd_{22.8}$, not exceeding a fraction of 2% in the whole temperature range covered in this work.

In Fig. 9, we show the quasilattice contribution to the specific heat of $Al_{70}Re_{8.6}Pd_{21.4}$ divided by T^3, versus temperature on double logarithmic scales. Analogous to $Al_{68.2}Mn_9Pd_{22.8}$, the specific-heat ratio C_{ph}/T^3 of $Al_{70}Re_{8.6}Pd_{21.4}$ shows a maximum at $T\approx25$ K. As mentioned above, the quasicrystal structure of icosahedral $Al_{70}Re_{8.6}Pd_{21.4}$ is similar to the structure of icosahedral $Al_{68.2}Mn_9Pd_{22.8}$. Although the atomic weight of Re is larger by a factor of 3 than the atomic weight of Mn, the ratio of the mass density ρ^R of $Al_{70}Re_{8.6}Pd_{21.4}$ to the mass density ρ^M of $Al_{68.2}Mn_9Pd_{22.8}$, $\rho^R/\rho^M=1.25$, is close to unity. Assuming that the elastic constants in $Al_{68.2}Mn_9Pd_{22.8}$ and $Al_{70}Re_{8.6}Pd_{21.4}$ quasicrystals are of similar magnitude we may estimate the sound velocity of icosahedral $Al_{70}Re_{8.6}Pd_{21.4}$. A simple renormalization of the average low-temperature sound velocity of icosahedral $Al_{68.2}Mn_9Pd_{22.8}$ (Ref. 15) using the mass density ratio mentioned above yields $v_s=3.7\times10^3$ m s^{-1} for icosahedral $Al_{70}Re_{8.6}Pd_{21.4}$. This value of the sound velocity is compatible with $C_D/T^3=2.2\times10^{-5}$ J g atom^{-1} K^{-4}, which is displayed as a horizontal solid line on the left margin of Fig. 9. The comparison with experiment again suggests a considerable excess specific heat C_{ex} at low temperatures in icosahedral $Al_{70}Re_{8.6}Pd_{21.4}$, as noticed before for $Al_{68.2}Mn_9Pd_{22.8}$.

In order to compare the quasilattice contributions to the specific heat $C_{ph}(T)$ of the two icosahedral quasicrystalline compounds $Al_{70}Re_{8.6}Pd_{21.4}$ and $Al_{68.2}Mn_9Pd_{22.8}$ in the temperature range where the maximum in C_{ph}/T^3 occurs, we plot the normalized specific heat $C_{ph}/(\beta T^3)$ versus the normalized temperature T/θ_D in the inset of Fig. 9. The maxima of the $C_{ph}/(\beta T^3)$ ratios for both icosahedral quasicrystals occur at the same reduced temperature, but the height of the maximum is distinctly larger in the case of $Al_{68.2}Mn_9Pd_{22.8}$, suggesting a stronger influence of a low-energy optical mode in Mn alloys than in the $Al_{70}Re_{8.6}Pd_{21.4}$ quasicrystal.

IV. CONCLUSIONS

The specific heat of both icosahedral $Al_{68.2}Mn_9Pd_{22.8}$ and $Al_{70}Re_{8.6}Pd_{21.4}$ has been measured in the temperature range between 1.6 K and room temperature. For both materials, the quasilattice contribution $C_{ph}(T)$ to the specific heat $C_p(T)$ is characterized by a broad maximum of the C_{ph}/T^3 vs T curve

at $T \approx 25$ K. Below 15 K, $C_{ph}(T)$ of both materials can adequately be described by an expression of the form $C_{ph} = \beta T^3 + \delta T^5$. The absolute value of the maximum of the C_{ph}/T^3 vs T curve of $Al_{68.2}Mn_9Pd_{22.8}$ can well be described by the presence of an optical mode at an energy of 10 meV.

At the lowest temperatures, the experimental cubic-in-T term to $C_{ph}(T)$ for both icosahedral Al-Mn-Pd and Al-Re-Pd quasicrystals is distinctly higher than the expected acoustic-phonon contribution, indicating a large excess specific heat C_{ex}. Part of this excess specific heat might be due to an unusually large cubic-in-T contribution of the electronic specific heat caused by a distinct and narrow minimum in the electronic DOS at the Fermi energy, but we estimate a possible contribution of that type to be quite small. The dominating part of the excess cubic-in-T term to the specific heat is most likely due to nonpropagating lattice excitations that do not manifest themselves in acoustical experiments.

ACKNOWLEDGMENT

This work was in part supported by the Schweizerische Nationalfonds zur Förderung der wissenschaftlichen Forschung.

[1] A. P. Tsai, A. Inoue, and T. Masumoto, Jpn. J. Appl. Phys., Part 2 **26**, L1505 (1987).
[2] A. P. Tsai, A. Inoue, and T. Masumoto, Jpn. J. Appl. Phys., Part 2 **27**, L1587 (1988).
[3] S. W. Kycia, A. I. Goldman, T. A. Lograsso, D. W. Delaney, D. Black, M. Sutton, E. Dufresne, R. Brüning, and B. Rodricks, Phys. Rev. B **48**, 3544 (1993).
[4] J. P. Lu, T. Odagaki, and J. L. Birman, Phys. Rev. B **33**, 4809 (1986).
[5] A. Y. Kitaev, JETP Lett. **48**, 298 (1988).
[6] S. E. Burkov, B. E. C. Koltenbah, and L. W. Bruch, Phys. Rev. B **53**, 14 179 (1996).
[7] P. A. Kalugin, M. A. Chernikov, A. Bianchi, and H. R. Ott, Phys. Rev. B **53**, 14 145 (1996).
[8] M. de Boissieu, M. Boudard, R. Bellissent, M. Quilichini, B. Hennion, R. Currat, A. I. Goldman, and C. Janot, J. Phys.: Condens. Matter **5**, 4945 (1993).
[9] M. Boudard, M. de Boissieu, S. Kycia, A. I. Goldman, B. Hennion, R. Bellissent, M. Quilichini, R. Currat, and C. Janot, J. Phys.: Condens. Matter **7**, 7299 (1995).
[10] H. Akiyama, Y. Honda, T. Hashimoto, K. Edagawa, and S. Takeuchi, Jpn. J. Appl. Phys., Part 2 **32**, L1003 (1993).
[11] M. A. Chernikov, A. Bernasconi, C. Beeli, A. Schilling, and H. R. Ott, Phys. Rev. B **48**, 3058 (1993).
[12] M. A. Chernikov, A. D. Bianchi, E. Felder, U. Gubler, and H. R. Ott, Europhys. Lett. **35**, 431 (1996).
[13] M. Boudard, E. Bourgeat-Lami, M. de Boissieu, C. Janot, M. Durand-Charre, H. Klein, M. Audier, and B. Hennion, Philos. Mag. Lett. **71**, 11 (1995).
[14] O. Jeandupeux, Ph.D. thesis, ETH Zürich, 1996.
[15] Y. Amazit, M. Fischer, B. Perrin, A. Zarembowitch, and M. de Boissieu, Europhys. Lett. **25**, 441 (1994).
[16] Y. Yokoyama, A. Inoue, and T. Masumoto, Mater. Trans., JIM **34**, 135 (1993).
[17] M. B. Hunt and H. R. Ott (unpublished).
[18] C. Janot, Phys. Rev. B **53**, 181 (1996).
[19] A. J. Sievers and S. Takeno, Phys. Rev. B **39**, 3374 (1989).
[20] S. Takeno and A. J. Sievers, Solid State Commun. **67**, 1023 (1988).
[21] K. Wang and P. Garoche, Phys. Rev. B **55**, 250 (1997).
[22] P. A. Bancel and P. A. Heiney, Phys. Rev. B **33**, 7917 (1986).
[23] J. Hafner and M. Krajci, Phys. Rev. Lett. **68**, 2321 (1992).
[24] T. Fujiwara, J. Non-Cryst. Solids **156-158**, 865 (1993).
[25] X. Wu, S. W. Kycia, C. G. Olson, P. J. Benning, A. I. Goldman, and D. W. Lynch, Phys. Rev. Lett. **75**, 4540 (1995).
[26] Z. M. Stadnik, D. Purdie, M. Garnier, Y. Baer, A. P. Tsai, A. Inoue, K. Edagawa, and S. Takeuchi, Phys. Rev. Lett. **77**, 1777 (1996).
[27] T. Fujiwara, T. Mitsui, S. Yamamoto, and G. T. de Laissardiere, in *Proceedings of the 5th International Conference on Quasicrystals, Avignon, France*, edited by C. Janot and R. Mosseri (World Scientific, Singapore, 1995), p. 393.
[28] E. A. Hill, T. C. Chang, Y. Wu, S. J. Poon, F. S. Pierce, and Z. M. Stadnik, Phys. Rev. B **49**, 8615 (1994).
[29] J. L. Gavilano, B. Ambrosini, P. Vonlanthen, M. A. Chernikov, and H. R. Ott, Phys. Rev. Lett. **79**, 3058 (1997).
[30] V. Simonet, F. Hippert, C. Gignoux, and C. Berger (unpublished).
[31] A. Kobayashi, S. Matsuo, T. Ishimasa, and H. Nakano, J. Phys.: Condens. Matter **9**, 3205 (1997).
[32] C. P. Slichter, in *Principles of Magnetic Resonance*, *Solid State Sciences 1*, edited by P. Fulde (Springer-Verlag, Berlin, 1989).
[33] R. O. Pohl, in *Amorphous Solids: Low-Temperature Properties*, Vol. 24 of Topics in Current Physics, edited by W. A. Phillips (Springer-Verlag, Berlin, 1981), p. 160.
[34] T. R. Sandin and P. H. Keesom, Phys. Rev. **177**, 1371 (1969).
[35] H. N. Pandey, Phys. Status Solidi **11**, 743 (1965).
[36] A. A. Maradudin, E. W. Montroll, G. H. Weiss, and I. P. Ipatova, in *Solid State Physics: Advances in Research and Applications*, edited by H. Ehrenreich, F. Seitz, and D. Turnbull (Academic, New York, 1971).
[37] G. Shirane and J. D. Axe, Phys. Rev. B **18**, 3742 (1978).
[38] B. M. Powell, P. Martel, and A. D. B. Woods, Phys. Rev. **171**, 727 (1968).
[39] W. Weber, Habilitation thesis, Universität Karlsruhe, 1984.
[40] F. W. de Wette and A. D. Kulkarni, Phys. Rev. B **46**, 14 922 (1992).
[41] M. de Boissieu (private communication).
[42] M. de Boissieu, F. Dugain, K. Hradil, K. Shibata, R. Currat, A. R. Kortan, A. P. Tsai, J. B. Suck, and F. Frey (private communication).
[43] V. F. Sears, Neutron News **3**, 26 (1992).
[44] J. B. Suck, J. Non-Cryst. Solids **153&154**, 573 (1993).
[45] M. Windisch, J. Hafner, M. Krajci, and M. Mihalkovic, Phys. Rev. B **49**, 8701 (1994).
[46] L. Degiorgi, M. A. Chernikov, C. Beeli, and H. R. Ott, Solid State Commun. **87**, 721 (1993).